

# 1 Proteome-wide comparison of tertiary protein structures reveal extensive 2 molecular mimicry in *Plasmodium*-human interactions

3 **Viraj Muthye<sup>1,2</sup>, James D. Wasmuth<sup>1,2\*</sup>**

4 <sup>1</sup> Faculty of Veterinary Medicine, University of Calgary, Calgary, Alberta, Canada

5 <sup>2</sup> Host-Parasite Interactions Research Training Network, University of Calgary, Calgary, Alberta,  
6 Canada

7 **\* Correspondence:**

8 Corresponding Author: James D. Wasmuth ([jwasmuth@ucalgary.ca](mailto:jwasmuth@ucalgary.ca))

9

10 **Keywords: molecular mimicry, malaria, plasmodium, AlphaFold, tertiary structure, host-**  
11 **parasite interactions**

## 12 **Abstract**

13 Molecular mimicry is a strategy used by parasites to escape the host immune system and successfully  
14 transmit to a new host. To date, high-throughput examples of molecular mimicry have been limited  
15 to comparing protein sequences. However, with advances in the prediction of tertiary structural  
16 models, led by Deepmind's AlphaFold, it is now possible to compare the tertiary structures of  
17 thousands of proteins from parasites and their hosts, to identify more subtle mimics. Here, we present  
18 the first proteome-level search for tertiary structure similarity between the proteins from *Plasmodium*  
19 *falciparum* and human. Of 206 *P. falciparum* proteins that have previously been proposed as  
20 mediators of *Plasmodium*-human interactions, we propose that seven evolved to molecularly mimic a  
21 human protein. By expanding the approach to all *P. falciparum* proteins, we identified a further 386  
22 potential mimics, with 51 proteins corroborated by additional biological data. These findings  
23 demonstrate a valuable application of AlphaFold-derived tertiary structural models, and we discuss  
24 key considerations for its effective use in other host-parasite systems.

25

## 26 **Introduction**

27 Parasites encounter host defenses at various points in their life cycle and employ a wide range of  
28 strategies for evading their host's immune response and successfully transmitting to a new host  
29 (Chulanetra & Chaicumpa, 2021). These host-parasite interactions may be mediated by parasite-  
30 derived molecules—including proteins, lipids, sugars—that unexpectedly resemble host-derived  
31 molecules. This is termed 'molecular mimicry', which was originally defined as the sharing of  
32 antigens between parasite and host (Damian, 1964). One of the earliest reports of molecular mimicry  
33 came from the parasitic nematode *Ascaris lumbricoides*, which possesses A- and B-like blood group  
34 antigens in its polysaccharides (Oliver-González, 1944). The definition of molecular mimicry has  
35 adapted to keep up with molecular and genomic technologies and is now widely considered to  
36 similarity between proteins at the level of primary structure (amino acid sequence) and tertiary  
37 structure (summarized in (Tayal et al., 2022)). An assumption is that molecular mimicry confers a  
38 fitness benefit to the pathogen. However, in immunology research, the term molecular mimicry can

39 be used to explain the cross-reactivity between exogenous and self-peptides and is the theoretical  
40 framework for understanding autoimmunity (Getts et al., 2013). Related to both these definitions,  
41 molecular mimicry might also result in heterologous immunity, in which the infection from one  
42 parasite protects against infection by other parasites with similar antigenic molecules (Balbin et al.,  
43 2023).

44 Here, our focus is molecular mimicry which likely confers a fitness advantage to the parasite, by  
45 either co-opting or disrupting the function of the mimicked host protein. Examples of molecular  
46 mimicry come from most branches of life. For instance, pathogenic bacterium *Escherichia coli*  
47 injects the TccP protein into host cells, which targets the polymerization of host actin. TccP contains  
48 multiple repeated motifs that mimic an internal regulatory element present in host N-WASP (neural  
49 Wiskott–Aldrich syndrome protein), which results in the activation of N-WASP (Sallee et al., 2008).  
50 This promotion of actin polymerization results in the creation of structures on epithelial cells that  
51 promote pathogen survival in the intestine. In another example, the myxoma virus decreases the  
52 number of activated macrophages by expressing its M128L protein on the host cell surface (Cameron  
53 et al., 2005). M128L shares significant sequence similarity with host CD47 and competes with it to  
54 bind with its receptor SIRP $\alpha$ . Within eukaryotic pathogens, the apicomplexan *Babesia microti*  
55 expresses the BmP53 protein which contains a domain that resembles thrombospondin (TSP1), a  
56 component of platelet cells (Mousa et al., 2017). The BmP53 TSP-1 is immunologically cross-  
57 reactive with human and it is proposed that BmP3 helps cloak the extra-cellular stages from the  
58 immune system.

59 To the best of our knowledge, the first study to identify host-parasite molecular mimicry at a  
60 genome-scale across multiple species was by Ludin and colleagues (Ludin et al., 2011). They  
61 considered the protein sequences from eight species of eukaryotic parasites, the host (human), and  
62 seven non-pathogenic, eukaryotic, negative control species. Their approach identified multiple  
63 potential instances of mimicry in these parasites. For example, they detected a 14 amino acid motif in  
64 multiple PfEMP1 proteins in *Plasmodium falciparum* that was identical to the heparin-binding  
65 domain in human vitronectin, a protein with multiple roles in human including cell-adhesion. The  
66 approach was repeated to find ninety-four potential mimicry proteins in a tapeworm–fish system  
67 (Hebert et al., 2015). It was also adapted and expanded for use with 62 pathogenic bacteria and  
68 identified approximately 100 potential mimics (Doxey & McConkey, 2013). These approaches rely  
69 on two proteins sharing enough sequence similarity to be detected by the sequence alignment  
70 software, *e.g.*, BLAST (Altschul et al., 1990). However, proteins may share too little sequence  
71 similarity. For instance, several viruses express proteins with tertiary structure similarity, but  
72 undetectable sequence similarity to human Bcl-2, and interfere with regulation of apoptosis  
73 (Kvansakul et al., 2007; Westphal et al., 2007). Similarly, in *Plasmodium falciparum*, a search of  
74 parasite proteins targeted to host extracellular vesicles revealed that at least eight shared unexpected  
75 and significant tertiary structure similarity with host proteins (Armijos-Jaramillo et al., 2021).

76 The opportunity to detect host-parasite mimicry at the level of tertiary structure has been limited by  
77 the number of available tertiary protein structures. Even for a parasite as important as *P. falciparum*,  
78 the protein databank (PDB) contains structures from less than 4% of the protein-coding genes in its  
79 genome (Table 1). We expect that most, if not all, other bacterial and eukaryotic pathogen species  
80 will have worse coverage. Proteome-wide searches for host-parasite molecular mimicry at the level  
81 of tertiary structure depended on *in silico* predictions that were of inconsistent quality (Armijos-  
82 Jaramillo et al., 2021). The prediction of tertiary protein structures from amino acid sequences has  
83 seen a much-publicised boon, in no small part to the development of AlphaFold (Ronneberger et al.,  
84 2021). In an early large-scale application, the AlphaFold Protein Structure Database (AFdb) provided

85 tertiary structure predictions for 16 model organisms and 32 pathogen species of global health  
86 concern (<https://alphafold.com>). Complementing the release of AlphaFold was Foldseek, a novel  
87 approach to aligning tertiary protein structures (van Kempen et al., 2022). Comparisons showed that  
88 FoldSeek was nearly 20,000 times faster than existing protein structure aligners while maintaining  
89 accuracy (but see (Holm, 2022)). These two major advances in structural bioinformatics—AlphaFold  
90 and Foldseek—have empowered us to investigate the usefulness of using tertiary protein structures  
91 for identifying instances of host-parasite molecular mimicry.

92 Our parasitic species of study is *Plasmodium falciparum*. While our understanding of the mediators  
93 of host-parasite interactions is limited, as the leading cause of severe malaria in humans, *P.*  
94 *falciparum* might represent the current pinnacle of our knowledge. Furthermore, the protein tertiary  
95 structures are complemented with a broad range of curated -omics datasets available on PlasmoDB,  
96 which can help with candidate prioritization (Amos et al., 2022; Aurrecochea et al., 2008). Proteins  
97 expressed by *P. falciparum* mediate interactions with its human host at multiple stages in its life  
98 cycle (Acharya et al., 2017). Molecular mimicry plays a role at both the liver and blood stages for  
99 immune evasion and cytoadherence. For instance, RIFIN, a prominent erythrocyte surface protein  
100 expressed by *P. falciparum*, binds to human LILRB1 which inhibits stimulation of the immune  
101 response. RIFIN does this by mimicking MHC Class I, the activating ligand of LILRBA (Harrison et  
102 al., 2020). Meanwhile, the circumsporozoite protein (CSP), which promotes invasion of human liver  
103 cells, has an 18 amino acid region that is similar to a cytoadhesive region in mammalian  
104 thrombospondin (Cerami et al., 1992; Robson et al., 1988).

105 In this study, our goal was to identify *P. falciparum* proteins which share tertiary structure similarity  
106 with human proteins but not detectable sequence similarity. First, we examined *P. falciparum*  
107 proteins which are known or have been implicated to directly interact with human biomolecules. We  
108 found new potential instances of molecular mimicry. Second, we extended our approach to consider  
109 all *P. falciparum* proteins and leveraged experimental datasets to filter the candidate mimics. Overall,  
110 our study highlights the advantages of using tertiary protein structures for identifying instances of  
111 molecular mimicry.

## 112 **Methods and Materials**

### 113 **2.1. Compiling the datasets of tertiary protein structures**

114 We downloaded tertiary protein structures for *Plasmodium falciparum* 3D7 (parasite), human (host),  
115 and 15 negative control species, *i.e.*, species that are not infected by *P. falciparum* (Table 1, File S1).  
116 Protein structures for these species were downloaded from two sources - 1) the RCSB Protein Data  
117 Bank (PDB) (experimentally-determined protein structures, last accessed 06/16/2022), and 2) the  
118 AlphaFold Protein Structure Database (AFdb) (computationally-predicted protein structures,  
119 <https://alphafold.ebi.ac.uk/>). The structures downloaded from both sources were processed before  
120 analysis (explained below).

121 **2.1.1. Processing the PDB structures:** Several PDB structures were composed of chains from  
122 multiple source organisms. We separated such structures into individual chains and extracted the  
123 appropriate chains corresponding to each species. For instance, the PDB structure 7F9N is composed  
124 of four chains (A to D), of which two chains (A and B) are from *P. falciparum* Rifin (RIF,  
125 PF3D7\_1000500) and two chains (C and D) are from the human leukocyte-associated  
126 immunoglobulin-like receptor 1 protein (LAIR1, Q6GTX8) (Figure 1A). We included only chains A  
127 and B for *P. falciparum*. Additionally, multiple structure chains were chimeric or ambiguous, *i.e.*,  
128 mapping to multiple source organisms. For instance, the PDB structure 4O2X has two chains (A and

129 B) which map to both *P. falciparum* and *Escherichia coli* strain K12. Such chains were discarded to  
130 not confound downstream analysis.

131 2.1.2. *Processing the AlphaFold structures*: AlphaFold assigns a score to each residue in the  
132 predicted structure called the ‘pLDDT’ score. This score is a measure of prediction confidence for  
133 that residue. The pLDDT scores range from 0 (low confidence of prediction) to 100 (high confidence  
134 of prediction). Regions with a pLDDT score above 90 are modeled with high accuracy, between 70-  
135 90 are modeled well, and 50-70 are modeled with low confidence. The AlphaFold database suggests  
136 that regions with pLDDT scores less than 50 should not be interpreted as this low score could be  
137 indicative of intrinsic protein disorder. For each AlphaFold structure, we calculated the proportion of  
138 the total residues with a pLDDT score of more than 70. We retained predicted structures with at least  
139 half the residues of the structure modeled with a pLDDT score above 70 (Figure 1B, File S1).

## 140 2.2. Identification of *Plasmodium falciparum* proteins known to interact with human molecules

141 We performed a literature survey to identify *P. falciparum* proteins that are known to interact with  
142 human molecules. We started with a review of *P. falciparum*-human protein interactions (Acharya et  
143 al., 2017). Then, we identified all abstracts on PubMed using the query - [‘plasmodium falciparum’  
144 AND ‘interact\*’ AND ‘protein\*’ AND ‘human\*’] from 2017 to 2022. This resulted in 648 abstracts  
145 (as of 8/8/2022 1:36 PM). We read all 648 abstracts to identify the *P. falciparum* proteins of interest.  
146 The PlasmoDB ID for each protein was mapped to Uniprot IDs using PlasmoDB (Release 52, 30  
147 August 2022). Three large gene families (PfEMP1, RIFIN, and STEVOR) play an important role in  
148 host-parasite interactions and pathogenesis in *P. falciparum*. Proteins belonging to these three  
149 families were downloaded from PlasmoDB.

## 150 2.3. Identification of sequence and structure similarity between *Plasmodium falciparum* and 151 human proteins

152 2.3.1. *Analysis of protein sequence similarity*: We analyzed sequence similarity between the proteins  
153 from *P. falciparum*, human, and 15 negative control species. We determined sequence similarity  
154 using three pairwise alignment search tools. SSEARCH36 implements the Smith-Waterman  
155 algorithm guaranteeing the optimal alignment. We used the following parameters for SSEARCH36  
156 from Fasta36 - ‘m 8 -s BL62 -f 12 -g 1’. BLASTP (Altschul et al., 1990) and DIAMOND (Buchfink  
157 et al., 2021) implement heuristic algorithms that are faster than SSEARCH36 but do not guarantee  
158 the optimal alignment. We used BLASTP with an e-value cut-off of  $1e^{-3}$  and performed an ultra-  
159 sensitive DIAMOND BLASTP search with the same e-value cut-off. For both aligners, we searched  
160 using the BLOSUM45 and BLOSUM62 substitution matrices. All other parameters were left as  
161 default. Additionally, we used OrthoFinder version 2.5.4 to identify groups of orthologous proteins  
162 between all the 17 species used in this study, using DIAMOND as the aligner (Emms & Kelly, 2019).  
163 The results of this analysis were used to identify human proteins that had orthologs in only the other  
164 three vertebrates used in this study (mouse, rat, and zebrafish).

165 2.3.2. *Analysis of protein structure similarity*: We aligned all *P. falciparum* structures to a database  
166 consisting of human structures and control structures. The structural aligner used was Foldseek v4  
167 (easy-search -s 9.5 --max-seqs 1000). We used an e-value cut-off of 0.01. Foldseek was also used to  
168 visualize structural alignments using the option ‘format-mode 3’.

169 2.3.3. *Expression analysis*: Expression analysis of *P. falciparum* proteins was carried out using the  
170 publicly available RNA-seq datasets available in PlasmoDB. We identified all *P. falciparum* proteins  
171 with expression in the 90<sup>th</sup> percentile in at least one of the stages in the intra-erythrocytic life cycle

172 (young ring 8 hpi, late ring/early trophozoite 16 hpi, mid trophozoite 24 hpi, late trophozoite 32 hpi,  
173 early schizont 40 hpi, schizont 44 hpi, late schizont 48 hpi, and purified merozoites 0 hpi) using data  
174 from (Wichers et al., 2019). We also identified all *P. falciparum* proteins with expression in the 90<sup>th</sup>  
175 percentile in the ring and/or sporozoite stage using data from (Zanghi et al., 2018).

## 176 **Results**

### 177 **3.1. Assembling and filtering the datasets of crystallised and computationally-predicted tertiary** 178 **protein structures**

179 We compiled tertiary protein structures from *Plasmodium falciparum* 3D7 (parasite), human (host),  
180 and 15 negative control species, those not infected by the parasite (Table 1, File S1). These structures  
181 were downloaded from the RCSB Protein Data Bank (PDB) and the AlphaFold Protein Structure  
182 database (AFdb). All AlphaFold-generated structures were filtered using the pLDDT score, a per-  
183 residue metric of the confidence of prediction accuracy. In line with the AlphaFold documentation,  
184 we considered structures to be high confidence if at least half their residues had a pLDDT score  
185 above 70. Through this filtering, we retained 56% of *P. falciparum* structures, 74% of human  
186 structures, and between 97% (*E. coli*) and 52% (*Oryza sativa*) for the control species (Table 1, Figure  
187 1B, File S1).

### 188 **3.2. Investigating the effect of the source of tertiary structures on Foldseek alignments**

189 We wanted to determine whether the source of the tertiary structure—crystallised (PDB) or  
190 computationally-predicted (AlphaFold)—affected the Foldseek search results. Following our  
191 filtering steps, 167 *P. falciparum* proteins were represented by structures from both PDB and  
192 AlphaFold and 159 aligned to at least one structure from the host and/or negative control species. For  
193 each of these 159 proteins, we compared the Foldseek results for their PDB and AlphaFold  
194 structures. For most of these proteins (107/159), the results for both PDB and AlphaFold queries  
195 agreed between 90 and 100%. For almost 10% of these proteins (15/159), the agreement between the  
196 results was lesser than 50% (File S2, Figure S1).

### 197 **3.3. Structural analysis of parasite proteins experimentally known to interact with human** 198 **proteins**

199 We performed a literature review and identified 74 *P. falciparum* proteins that interact with human  
200 molecules at various stages in its life-cycle (File S3). We also included three large *P. falciparum*  
201 gene families which are thought to play a role in parasite virulence—PfEMP1 (61 proteins), RIFIN  
202 (158 proteins), and STEVOR (32 proteins) (File S3). Overall, 206 of these proteins were represented  
203 by at least one structure in our database of PDB and high-quality AlphaFold structures. To  
204 understand whether molecular mimicry plays a role in how these proteins interact with the host, we  
205 asked the question: do these 206 *P. falciparum* proteins share sequence and/or tertiary structural  
206 similarity with human proteins?

207 We found that 31 proteins (15%) shared structural similarity with at least one human protein. Of  
208 these, three proteins aligned to human proteins which were restricted in vertebrates at the sequence-  
209 level (orthologs in only mouse, rat, and/or zebrafish). They were the parasite circumsporozoite  
210 protein (CSP, PF3D7\_0304600) and two PfEMP1 proteins (PF3D7\_0800100 and PF3D7\_0617400).  
211 CSP was aligned to human thrombospondin (TSP1, P07996). Interestingly, as per previous sequence-  
212 based approaches, CSP mimics a cytoadhesive region in mammalian thrombospondin (Cerami et al.,  
213 1992; Robson et al., 1988).

214 Next, from these 31 proteins, we removed all parasite proteins which shared sequence similarity with  
215 human proteins – 15, 16, and 15 proteins aligned to human proteins by BLASTP, DIAMOND, and  
216 SSEARCH36 respectively (Figure 2A). Only 11 of these 31 *P. falciparum* proteins shared structure  
217 similarity but not sequence similarity to human proteins (Figure 2A). For these 11 proteins, we  
218 visually inspected their structural alignments with human proteins (File S4) and here we present the  
219 biological relevance of their interactions for seven proteins.

220 Three *PfEMP1* proteins: *P. falciparum* erythrocyte membrane protein 1 (PfEMP1) proteins primarily  
221 function in adhesion of infected erythrocytes to the vasculature. Here, our results suggest potential  
222 novel functions for three members of this large gene-family. Of the 61 PfEMP1 family proteins  
223 analyzed in this study, six shared structural similarity, but not sequence similarity, to human proteins.  
224 Two PfEMP1 proteins (PF3D7\_0100300 and PF3D7\_0600400) were similar to the human tyrosine-  
225 protein phosphatase non-receptor type 23 (PTPN23). Additionally, PTPN23 was the second-best  
226 Foldseek alignment for one more PfEMP1 protein (PF3D7\_0937600). Interestingly, PTPN23  
227 interacts with six human proteins that function in cytokine signaling (PTPN4, PTPN9, PTPN13,  
228 PTPN14, and GRAP2), suggesting that the three PfEMP1 proteins could be involved in immune  
229 modulation of the host by interfering in cytokine signaling (Figure S2).

230 *AMA1*: The apical membrane antigen (AMA1, PF3D7\_1133400) interacts with the host erythrocyte  
231 membrane transport protein Kx protein (Kato et al., 2005) and is considered a potential vaccine target  
232 (Remarque et al., 2008). AMA1 has multiple crystallised structures, in addition to its AlphaFold  
233 prediction. AMA1 was aligned to human plasma kallikrein protein (KLKB1), a member of the  
234 plasma kallikrein–kinin system (KKS) in human. KKS proteins are known to interact with immune  
235 and complement systems (Wu, 2015). KLKB1 has also been implicated in the renin-angiotensin  
236 system (RAS), where it converts prorenin to renin (Schmaier, 2003). Some studies have reported an  
237 anti-malarial effect for RAS components. For instance, angiotensin II (which is formed by the  
238 cleavage of angiotensin to angiotensin I by renin and conversion to angiotensin II by angiotensin-  
239 converting enzyme) has been shown to inhibit different stages of multiple *Plasmodium* species and  
240 also reduce cerebral malaria pathogenesis (reviewed in (De et al., 2022)). We propose that AMA1  
241 mimics KLKB1 to prevent the formation of angiotensin II by inhibiting renin activity.

242 *P38*: The 6-cysteine protein/merozoite surface protein P38 (P38, PF3D7\_0508000) functions in red-  
243 blood cell invasion and binds to human glycophorin-A (GLPA, P02724) (Paul et al., 2017). We  
244 found that P38 was structurally similar to human titin (TTN, Q8WZ42) and fibroblast growth factor  
245 receptor 1 (FGFR1, P11362). The region from FGFR1 similar to P38 contained the two Ig-like  
246 protein domains ‘Immunoglobulin I-set domain (PF07679)’ and the ‘Immunoglobulin domain  
247 (PF00047)’. The regions similar to P38 from TTN also contained immunoglobulin-like domains. The  
248 ‘Immunoglobulin I-set domain’ are present in several adhesion proteins in human, where Ig-like  
249 domains play an important role in homophilic cell adhesion (Leshchynska & Sytnyk, 2016). This  
250 suggests that P38, in addition to binding to GLPA, functions in adhesion owing to its similarity to the  
251 Ig-like domains.

252 *CyPRA*: The cysteine-rich protective antigen (CyPRA, PF3D7\_0423800) interacts with two other  
253 parasite proteins (PfRH5 and PfRipr) to form a complex on the surface of an invading merozoite and  
254 is considered a potential vaccine target (Ragotte et al., 2020). CyPRA was represented by multiple  
255 structures from both the PDB and AFdb. The only human protein which shared tertiary structural  
256 similarity to both PDB and AlphaFold structures was the V(D)J recombination-activating protein 2  
257 (RAG2, P55895) (Figure 2B). We identified the human interacting partners of RAG2 using StringDB  
258 (Figure S3). Seven interactors functioned in ‘signaling by Interleukins’, of which four were involved

259 in ‘MAPK family signaling cascades’. The next best alignment was mitogen-activated protein kinase  
260 kinase kinase kinase 4 (MAP4K4, O95819), which also functions in the MAPK signaling. Thus, in  
261 addition to its key role in red blood cell invasion, structural similarity analysis suggests a possible  
262 novel role for CyPRA in modulating the host MAPK signaling pathway.

263 *SHLP2*: In at least one instance, our approach identified structural similarity in protein domains  
264 between the parasite and human proteins, which was missed by sequence similarity searches.  
265 Foldseek aligned the region containing the ‘Metallophos’ protein domain between the parasite  
266 protein ‘Shewanella-like protein phosphatase 2’ (SHLP2, PF3D7\_1206000) and the human  
267 phosphatase ‘Serine/threonine-protein phosphatase with EF-hands 1’ (PPEF1, O14829).

### 268 **3.4. Large-scale analysis of the structural similarity between *Plasmodium falciparum* and** 269 **human proteins**

270 The previous section shows that our approach can identify instances of molecular mimicry which  
271 mediate host-*Plasmodium* interactions. This motivated us to extend the approach to search all tertiary  
272 structures from *P. falciparum* against a database of 415,164 structures from human and the 15  
273 negative control species. Of the parasite’s 4,326 tertiary structures, 3,649 (84%) were aligned to a  
274 structure from human and/or negative control species, and 3,350 (77%) could be aligned to a human  
275 structure.

276 Of these 3,350 structures, 59 structures were similar to only vertebrate proteins, and 27 aligned to  
277 only mammalian structures. Only eight structures aligned exclusively to a human structure. We  
278 further examined the structural alignments of these eight structures and identified potential novel  
279 biological functions for some of them. As mentioned above (section 3.3), the parasite protein CSP  
280 was aligned to human thrombospondin-1. The parasite protein 40S ribosomal protein S30 (RPS30,  
281 PF3D7\_0219200) was shared tertiary structural similarity to human FAU ubiquitin-like and  
282 ribosomal protein S30 (FAU, P62861), which functions in apoptosis (Pickard et al., 2011) and is  
283 mapped to the GO term ‘innate immune response in mucosa’ in UniProt. This suggests that RPS30  
284 could provide a biological advantage to *P. falciparum* by modulating the human immune response.  
285 The perforin-like protein 3 (PLP3, PF3D7\_0923300) was aligned to human macrophage-expressed  
286 gene 1 (MPEG1, Q2M385), which functions in the host innate immune response. While PLP is  
287 expressed in both sexual and asexual stages of the parasite, it primarily functions in the mosquito-  
288 stage of the parasite (S. Garg et al., 2020). Thus, it is possible that PLP3 has an additional function in  
289 the human host to avoid the immune response.

290 Nearly one-fifth of the *P. falciparum* proteins that shared structural similarity to human proteins  
291 (386/2,120) had no detectable sequence similarity to a human protein (File S5). On average, 352 *P.*  
292 *falciparum* proteins had structural similarity but no sequence similarity to the control proteins.  
293 Overall, such *P. falciparum* proteins with structure similarity but not sequence similarity were not the  
294 same for each of these 16 species (Figure S4).

295 To prioritise the proteins, we categorized them with available annotations from PlasmoDB. Category  
296 1 was predicted function, where the top scoring alignment was with a human protein with a GO term  
297 of interest—‘immune system process’, ‘cell adhesion’, ‘cytoskeleton’, or ‘signalling’. Category 2  
298 was likely export from the cell, where the *P. falciparum* protein was predicted to contain a signal  
299 peptide. Category 3 was the gene’s expression, where we selected proteins whose genes was  
300 expressed in the 90<sup>th</sup> percentile in at least one of the human life-cycle stages of the parasite—  
301 sporozoite and ring—or one of the intraerythrocytic stages (Wichers et al., 2019; Zanghi et al., 2018).

302 A total of 169 *P. falciparum* proteins could be placed in at least one of the categories, with 97  
303 proteins in category 1, 43 in category 2, 95 in category 3, 38 in two categories, and 13 proteins in all  
304 three categories (Figure S5, Table 2). Seven of the nine top human proteins aligned to these *P.*  
305 *falciparum* 13 proteins were taxonomically restricted to vertebrates.

306 The 51 *P. falciparum* proteins present in more than category represent instances of mimicry (File  
307 S6). Here, we present the biological relevance of a subset of these proteins. The four 6-cysteine  
308 proteins present in these 13 proteins are one of the most abundant surface antigens in the *P.*  
309 *falciparum* (Lyons et al., 2022) and have been attributed to virulence in related parasites (Wasmuth et  
310 al., 2012). These are promising candidates for mediators of host-parasite interactions. The first  
311 example was the P92/merozoite surface protein (P92, PF3D7\_1364100), which interacts with human  
312 Factor H to downregulate the alternative complement pathway (Kennedy et al., 2016). We found that  
313 P92 shared structural similarity to human T-cell surface protein tactile (CD96, P40200), a  
314 transmembrane protein that is expressed by both T and NK cells (Georgiev et al., 2018).  
315 Interestingly, multiple roles for NK cells have been proposed at different stages of *P. falciparum*  
316 infection, including cytotoxic activity against the erythrocyte and hepatocyte stages (reviewed in  
317 (Wolf et al., 2017)). Additionally, six of the proteins CD96 interacts with function in immune  
318 response (GO:0006955) (Figure S6). Therefore, it is possible that P92 assists parasite infection by  
319 modulating the human immune response.

320 The second and third examples are the 6-cysteine protein P12/merozoite surface protein P12 (P12,  
321 PF3D7\_0612700) and merozoite surface protein 41 (P41, PF3D7\_0404900), which were similar to  
322 human polymeric immunoglobulin receptor PIGR (PIGR, P01833). PIGR is a known receptor for  
323 immunoglobulin M (IgM) (Pleass et al., 2016) and IgM is known to block the invasion of red blood  
324 cells by *Plasmodium* merozoites (Oyong et al., 2019). In fact, four other *P. falciparum* proteins -  
325 VAR2CSA, TM284VAR1, DBLMSP, and DBLMSP2, bind to IgM and affect IgM-mediated  
326 complement activation for evading the human immune response (Ji et al., 2022). Our structure-based  
327 approach suggests a similar role for P12 and P41. The fourth example is sporozoite invasion-  
328 associated protein 1 (SIAP1, PF3D7\_0408600), which was aligned to human collagen alpha-1(VII)  
329 chain (COL7A1, Q02388). StringDB identified seven proteins that interact with COL7A1 and are  
330 mapped to the GO term 'cell adhesion' (GO:0007155) (Figure S7). Additionally, six proteins were  
331 mapped to the KEGG pathway 'ECM-receptor interaction' (hsa04512). Thus, we posit that SIAP1  
332 could play a role in adhesion of the parasite to the host extracellular matrix.

333 An additional 35 parasite proteins were present in two of the three categories listed above. All  
334 warrant further investigation, but two are noteworthy. First, the sporozoite surface protein P36  
335 (PF3D7\_0404500) was similar to human PIGR, like two other members of the 6-cysteine protein  
336 family - P12 and P41. In fact, P36 was aligned to a similar region in PIGR compared to P12 and P41.  
337 This suggests that P12 potentially binds to IgM and helps the parasite evade the host immune  
338 response. When we analyzed all Foldseek alignments (not just the best hits), we found that an  
339 additional four 6-cysteine proteins were also similar to PIGR - 6-cysteine protein P12p (P12p,  
340 PF3D7\_0612800), 6-cysteine protein P52 (P52, PF3D7\_0404500), 6-cysteine protein (P48/45,  
341 PF3D7\_1346700), and 6-cysteine protein P47 (P47, PF3D7\_1346800). Second, the LamG domain-  
342 containing protein (PF3D7\_0723200), which possesses a signal peptide, shared tertiary structure  
343 similarity to the human adhesion G-protein coupled receptor V1 (ADGRV1, Q8WXG9), a cell-  
344 surface protein involved in cell adhesion. StringDB found that five of its interacting partners function  
345 in 'cell-cell adhesion' (GO:0098609), suggesting that the *P. falciparum* protein assists parasite  
346 infection and survival by functioning in cell adhesion.



## 347 Discussion

348 In this study, we present, to the best of our knowledge, the first genome-scale search of tertiary  
349 structural similarity between *P. falciparum* proteins and human proteins. We demonstrate the  
350 usefulness of our approach by showing that approximately 7% of the *P. falciparum* proteins had  
351 similarity to human proteins that could be detected only at the level of tertiary structure, and not  
352 primary sequence. Using available molecular and -omics datasets from PlasmoDB, we shortlisted a  
353 set of 51 instances of mimicry that are candidate mediators of host-parasite interactions.

354 We compared whether the source of the structural model made a difference. It made a considerable  
355 difference (<50% agreement) for 10% of proteins. We emphasize that this is for AlphaFold structures  
356 that were filtered for high confidence; we anticipate that for lower confidence AlphaFold structures,  
357 an agreement with a PDB structure would be worse. Improvement in the AlphaFold software and its  
358 evolutionary models will lead to better structural models, but users must remain vigilant of accuracy  
359 metrics when using this promising resource. If a particular gene of interest has a protein structural  
360 model available in the PDB, we recommend incorporating it in the analysis. A recent notable study  
361 attempted to overcome this challenge by improving AlphaFold predictions for two parasites -  
362 *Trypanosoma cruzi* and *Leishmania infantum* (Wheeler, 2021). They attributed the poor accuracy of  
363 tertiary structure prediction for several parasite proteins to the low number of representative parasite  
364 sequences used to predict them and demonstrated that they could improve the AlphaFold predictions  
365 by increasing the number of parasite sequences used to model these structures.

366 We validated our approach on known mediators of host-parasite interactions and we identified known  
367 similarity between CSP and thrombospondin-1. We also identified potential novel functions of  
368 multiple parasite proteins, which improves our understanding of existing *P. falciparum*-human  
369 interactions. One promising example involves multiple members of the 6-cysteine proteins found in  
370 *P. falciparum*. Members of this gene-family are expressed in multiple stages of the *P. falciparum*  
371 life-cycle in both the hosts (Lyons et al., 2022). Interestingly, while several members of this family  
372 have been implicated in critical functions like immune-evasion and host cell invasion, the precise  
373 roles for several of these proteins, like P12, P12p, P38, and P41, remain unknown (Lyons et al.,  
374 2022). Therefore, our structure-similarity-based approach improved our knowledge of how some of  
375 these proteins contribute to immune evasion, by identifying a potential binding-partner (IgM) and  
376 function for these proteins.

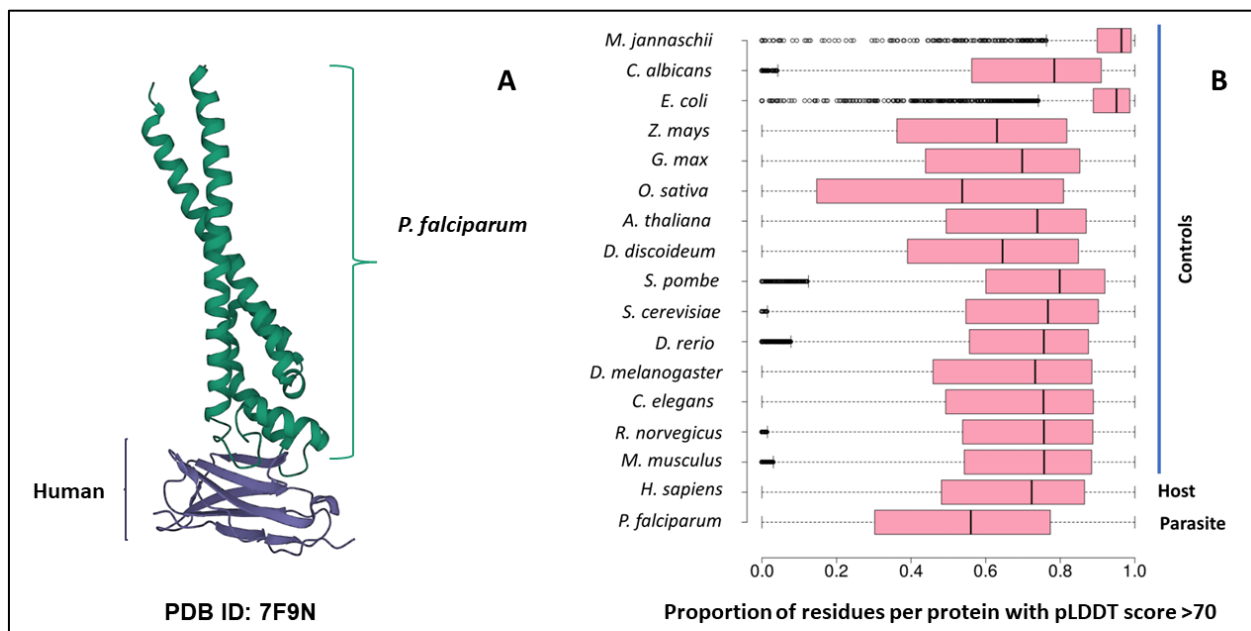
377 There are four important points to consider when interpreting the results of this analysis. First, we  
378 noticed that the number of parasite proteins with structural similarity, but not sequence similarity, to  
379 human and negative control proteins was similar for the majority of species studied. Some these  
380 would be distant homologs which are not detected by sequence-based tools employed in this study.  
381 Indeed, the failure of homology detection has been shown to be one of the important reasons for the  
382 presence of lineage-specific genes (Weisman et al., 2020). In fact, multiple studies have  
383 demonstrated the effectiveness of using structure data to identify distant homologs that are missed by  
384 sequence-based approaches (Andorf et al., 2022; Monzon et al., 2022). Other proteins, however,  
385 would represent false-positives of our approach based on our definition of ‘molecular mimics’, in  
386 which we define that a mimic confers benefit to the parasite. To this end, we used experimental data  
387 on *P. falciparum* from PDB to shortlist 46 proteins in *P. falciparum* that are structurally similar to  
388 human proteins and have a high probability of benefiting the parasite via its mimicry of a human  
389 protein. It is important to note that the majority of parasites lack similar resources, making such an  
390 analysis for them problematic. This highlights the need to develop resources, like PlasmoDB, for  
391 other parasites of global health concern.

392 Second, since we discarded AlphaFold predictions with low prediction accuracy, we ended up  
393 removing structures with a high level of intrinsic protein disorder. This is unfortunate as instances of  
394 mimicry have been identified in such disordered regions. For example, it has been proposed that  
395 viruses modulate host cellular processes by mimicking regions in disordered regions (Dolan et al.,  
396 2015; A. Garg et al., 2022; Xue et al., 2014). Such mimicking regions in disordered regions can be  
397 potentially identified by supplementing our structure-based approach with a *k*-mer based approach.

398 Third, the influence of the structure aligner must be considered. Foldseek is orders of magnitude  
399 faster than other currently available structural aligners and the only software that allows, in a  
400 reasonable time, the type of comparison presented here. However, the trade-off in terms of accuracy  
401 is a matter of debate (Holm, 2022; van Kempen et al., 2022). The alignment speed of DALI makes it  
402 unsuitable for large-scale structural similarity searches.

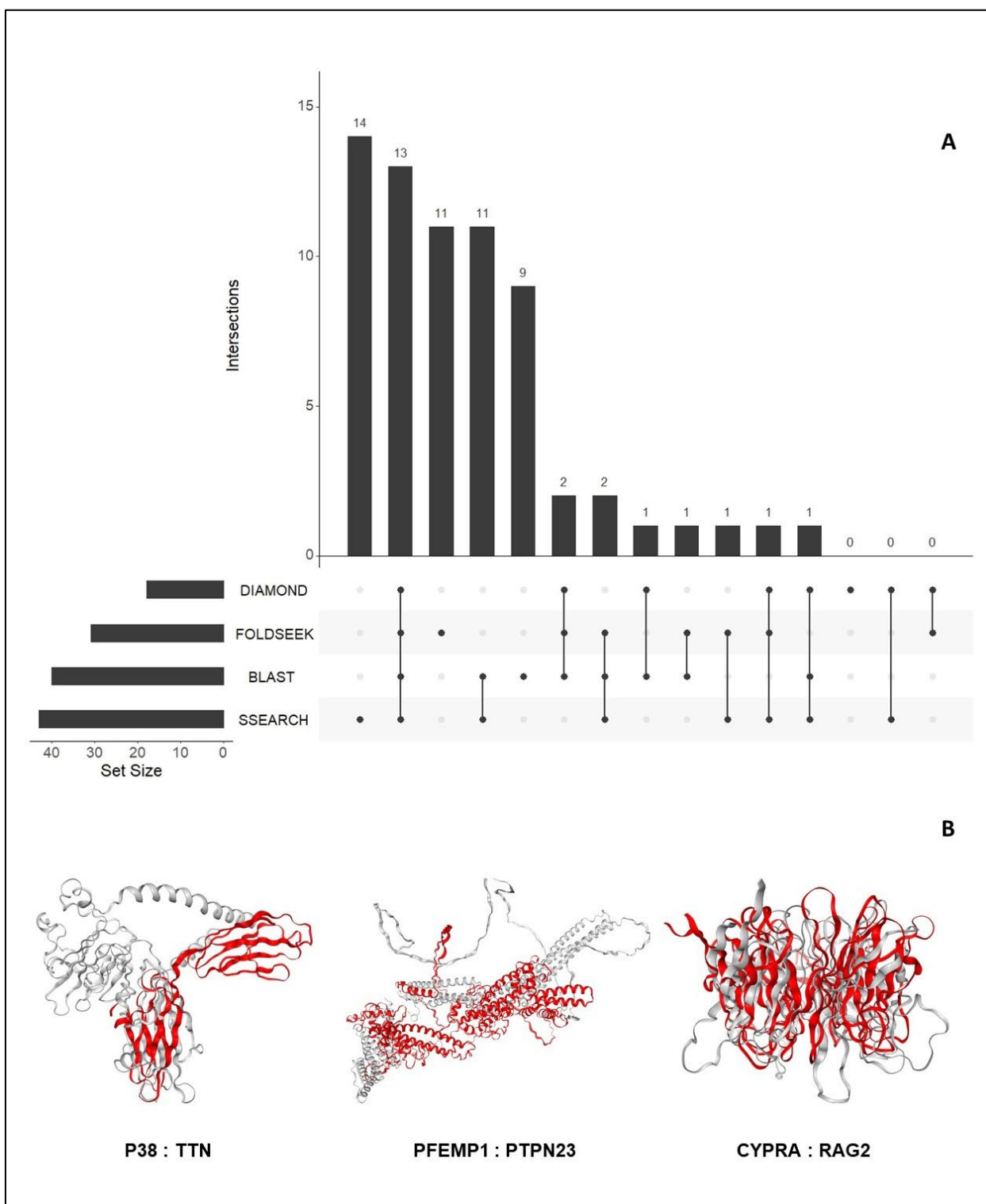
403 In conclusion, we present, to the best of our knowledge, the first genome-level search of tertiary  
404 structure similarity between *P. falciparum* and human proteins and use the results of the search to  
405 identify instances of molecular mimicry between the parasite and the host. The extensive  
406 experimental data for *P. falciparum* on PlasmoDB guided our efforts to unearth the biological  
407 relevance of the identified similarities. The list of *P. falciparum* mimics catalogued in our study  
408 represent excellent candidates for experimental validation. Our results help further our insights into  
409 the molecular nature of *Plasmodium*-human interactions and will be important to inform efforts on  
410 developing vaccines and therapeutics against malaria.

## 411 Figures



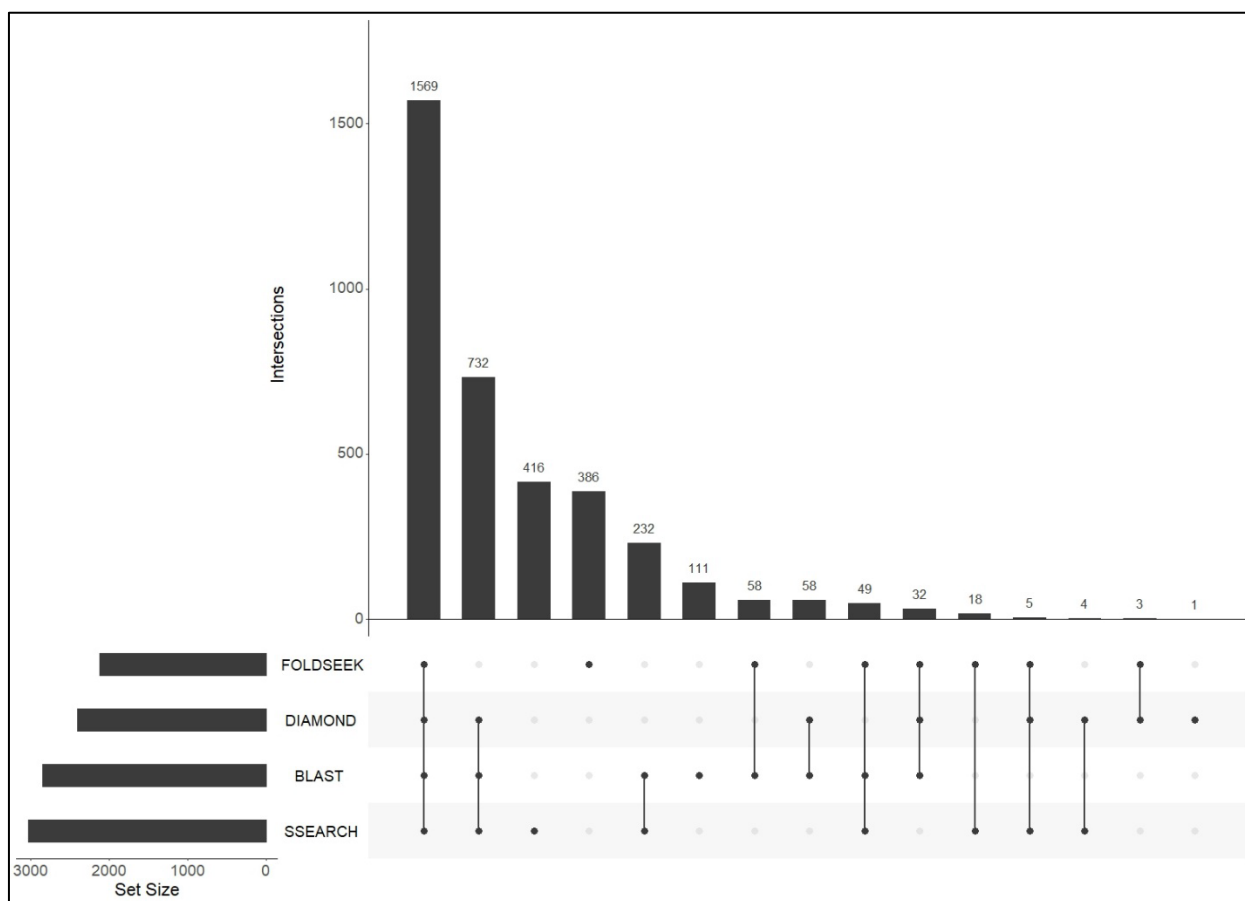
412

413 **Figure 1** A) The 7F9N protein tertiary structure from the RCSB Protein Data Bank. The chains from  
414 the *P. falciparum* RIFIN protein (RIF, PF3D7\_1000500) are colored in green and the chains from the  
415 human LAIR protein (LAIR1, Q6GTX8) are colored in purple. B) Box-plot representing the overall  
416 prediction accuracy for each protein in the AFdb. Each point in this distribution represents the  
417 proportion of all residues with a pLDDT score above 70 for one AlphaFold structure. The median  
418 value is the parallel bar within the box. The limits of the box are the 25<sup>th</sup> and 75<sup>th</sup> percentiles, the  
419 whiskers extend 1.5 times the interquartile range, and the dots are the outliers.



420

421 **Figure 2** A) An UpSet plot of the 206 parasite proteins that interact with human molecules and are  
 422 represented by at least one structure in our database. This plot displays the number of these  
 423 interacting parasite proteins aligned to human proteins by DIAMOND, BLAST, Foldseek, and/or  
 424 SSEARCH36. B) Tertiary structure alignments of the parasite structures (gray) and human structures  
 425 (red). These alignments were generated and visualized using Foldseek.



426

427 **Figure 3** An UpSet plot of all *Plasmodium falciparum* proteins which were aligned to human  
 428 proteins by Foldseek, DIAMOND, BLASTP, and/or SSEARCH36.

429 **Tables**

430 **Table 1** The number of tertiary protein structures for each species used in this study. Structures were  
 431 downloaded from two sources - the AlphaFold Protein structure Database (AFdb) and the RCSB Protein Data  
 432 Bank (PDB). These structures were filtered according to the steps outlined in Section 2.1. The number protein-  
 433 coding genes were taken from UniProt.

Category	Species	Protein-coding genes in UniProt	AlphaFold structures (that passed filtering)	PDB chains	Uniprot proteins mapping to PDB structures	Total tertiary structures	Uniprot proteins with tertiary structures
Control	<i>Arabidopsis thaliana</i>	27,498	20,460	4,560	899	25,020	20,612
Control	<i>Caenorhabditis elegans</i>	19,838	14,683	1,036	231	14,968	14,736

Control	<i>Candida albicans</i> SC5314 / ATCC MYA-2876	6,759	4,777	285	62	5,813	4,790
Control	<i>Danio rerio</i>	26,355	19,541	1,026	157	20,567	19,627
Control	<i>Dictyostelium</i> <i>discoideum</i>	12,727	8,259	345	55	8,604	8,266
Control	<i>Drosophila</i> <i>melanogaster</i>	13,821	9,685	2,624	505	12,309	9,877
Control	<i>Escherichia coli</i> strain K12	4,402	4,220	11,242	1,087	15,462	4,332
Control	<i>Glycine max</i>	55,855	39,168	314	42	39,482	39,180
Host	<i>Homo sapiens</i>	20,594	17,226	125,073	8,215	142,299	17,568
Control	<i>Methanocaldococ</i> <i>cus jannaschii</i> strain DSM 2661	1,787	1,708	511	99	2,219	1,709
Control	<i>Mus musculus</i>	21,968	16,911	13,419	2,227	30,330	17,562
Control	<i>Oryza sativa</i> <i>subsp. japonica</i>	43,673	22,852	410	77	23,262	22,873
Parasite	<i>Plasmodium</i> <i>falciparum</i> isolate 3D7	5,372	2,909	1,417	207	4,326	2,949
Control	<i>Rattus norvegicus</i>	22,816	16,555	7,512	668	24,067	16,705
Control	<i>Saccharomyces</i> <i>cerevisiae</i> strain ATCC 204508 / S288c	6,060	4,745	15,228	1,215	19,973	4,878
Control	<i>Schizosaccharomy</i> <i>ces pombe</i> strain 972 / ATCC 24843	5,122	4,224	1,388	295	5,612	4,260
Control	<i>Zea mays</i>	39,208	24,721	456	94	25,177	24,757

434

435 **Table 2** Top Foldseek alignments for the 13 *P. falciparum* proteins that were present in all three categories  
 436 outlined in section 3.4.

<i>P. falciparum</i> protein  (UniProt ID / PlasmoDB ID)	Protein name	Human protein	Protein name	<i>P. falciparum</i> structure	Human structure	e-value	Foldseek score
A0A144A2G5/ PF3D7_111670 0	dipeptidyl aminopeptidase 1	P53634	Dipeptidyl peptidase 1	AF-A0A144A2G5-F1-model_v2.pdb.gz	AF-P53634-F1-model_v2.pdb.gz	3.91E-28	761
C0H473/ PF3D7_031400 0	HSP20-like chaperone	Q9P035	Very-long-chain (3R)-3-hydroxyacyl-CoA dehydratase 3	AF-C0H473-F1-model_v2.pdb.gz	AF-Q9P035-F1-model_v2.pdb.gz	1.71E-09	314
C6KSX0/ PF3D7_061270 0	6-cysteine protein P12	P01833	Polymeric immunoglobulin receptor	AF-C6KSX0-F1-model_v2.pdb.gz	6UE7_C.pdb.gz	3.44E-07	84
Q8I1Y0/ PF3D7_040490 0	6-cysteine protein P41	P01833	Polymeric immunoglobulin receptor	4YS4_A.pdb.gz	5D4K_B.pdb.gz	1.11E-04	67
Q8I395/ PF3D7_090540 0	high molecular weight rhoptry protein 3	Q5TBA9	Protein furry homolog	AF-Q8I395-F1-model_v2.pdb.gz	AF-Q5TBA9-F10-model_v2.pdb.gz	5.06E-03	48
Q8I423/ PF3D7_050800 0	6-cysteine protein P38	Q8WZ42	Titin	AF-Q8I423-F1-model_v2.pdb.gz	AF-Q8WZ42-F19-model_v2.pdb.gz	8.90E-06	79
Q8I4R4/ PF3D7_125220 0	chitinase	P36222	Chitinase-3-like protein 1	AF-Q8I4R4-F1-model_v2.pdb.gz	1HJW_B.pdb.gz	1.15E-06	169
Q8IAV9/ PF3D7_081230 0	sporozoite surface protein 3	O75161	Nephrocystin-4	AF-Q8IAV9-F1-model_v2.pdb.gz	AF-O75161-F1-model_v2.pdb.gz	2.43E-05	62

Q8ID66/ PF3D7_136410 0	6-cysteine protein P92	P40200	T-cell surface protein tactile	AF-Q8ID66- F1- model_v2.pdb.g z	AF-P40200-F1- model_v2.pdb.g z	2.01E-06	71
Q8IFM8/ PF3D7_042380 0	cysteine-rich protective antigen	P55895	V(D)J recombination- activating protein 2	AF-Q8IFM8- F1- model_v2.pdb.g z	AF-P55895-F1- model_v2.pdb.g z	7.19E-08	184
Q8IIU7/ PF3D7_110560 0	translocon component PTEX88	Q16531	DNA damage- binding protein 1	AF-Q8IIU7-F1- model_v2.pdb.g z	5V30_A.pdb.g z	1.42E-10	156
Q8IM47/ PF3D7_140470 0	cysteine-rich small secreted protein CSS	O75161	Nephrocystin-4	AF-Q8IM47- F1- model_v2.pdb.g z	AF-O75161-F1- model_v2.pdb.g z	3.57E-05	68
Q9U0K0/ PF3D7_040860 0	sporozoite invasion- associated protein 1	Q02388	Collagen alpha-1(VII) chain	AF-Q9U0K0- F1- model_v2.pdb.g z	AF-Q02388-F2- model_v2.pdb.g z	7.23E-03	38

437

#### 438 **Conflict of Interest**

439 The authors declare that the research was conducted in the absence of any commercial or financial  
440 relationships that could be construed as a potential conflict of interest.

#### 441 **Author Contributions**

442 Conceived and designed the analyses: VM & JW. Performed the analyses: VM. Wrote the  
443 manuscript: VM & JW.

#### 444 **Funding**

445 This work was supported by Natural Sciences and Engineering Research Council of Canada  
446 (NSERC) Discovery Grant (#04589-2020) to JDW and an Eyes High Postdoctoral recruitment  
447 scholarship to VM. The funders had no role in study design, data collection and analysis, decision to  
448 publish, or preparation of the manuscript.

#### 449 **Acknowledgments**

450 We thank Kaylee Rich and Dr. Constance Finney for their discussions on various aspects of the  
451 manuscript. We acknowledge the high-performance computing resources made available by the  
452 Faculty of Veterinary Medicine and Research Computing at the University of Calgary.

#### 453 **References**

- 454 Acharya, P., Garg, M., Kumar, P., Munjal, A., & Raja, K. D. (2017). Host–Parasite Interactions in  
455 Human Malaria: Clinical Implications of Basic Research. *Frontiers in Microbiology*, 8.  
456 <https://doi.org/10.3389/fmicb.2017.00889>
- 457 Altschul, S. F., Gish, W., Miller, W., Myers, E. W., & Lipman, D. J. (1990). Basic local alignment  
458 search tool. *Journal of Molecular Biology*, 215(3), 403–410. <https://doi.org/10.1016/S0022->  
459 2836(05)80360-2
- 460 Amos, B., Aurrecochea, C., Barba, M., Barreto, A., Basenko, E. Y., Bazant, W., Belnap, R.,  
461 Blevins, A. S., Böhme, U., Brestelli, J., Brunk, B. P., Caddick, M., Callan, D., Campbell, L.,  
462 Christensen, M. B., Christophides, G. K., Crouch, K., Davis, K., DeBarry, J., ... Zheng, J. (2022).  
463 VEuPathDB: the eukaryotic pathogen, vector and host bioinformatics resource center. *Nucleic Acids*  
464 *Research*, 50(D1), D898–D911. <https://doi.org/10.1093/nar/gkab929>
- 465 Andorf, C. M., Sen, S., Hayford, R. K., Portwood, J. L., Cannon, E. K., Harper, L. C., Gardiner, J.  
466 M., Sen, T. Z., & Woodhouse, M. R. (2022). FASSO: An AlphaFold based method to assign  
467 functional annotations by combining sequence and structure orthology. *BioRxiv*.  
468 <https://doi.org/10.1101/2022.11.10.516002>
- 469 Armijos-Jaramillo, V., Mosquera, A., Rojas, B., & Tejera, E. (2021). The search for molecular  
470 mimicry in proteins carried by extracellular vesicles secreted by cells infected with *Plasmodium*  
471 *falciparum*. *Communicative & Integrative Biology*, 14(1), 212–220.  
472 <https://doi.org/10.1080/19420889.2021.1972523>
- 473 Aurrecochea, C., Brestelli, J., Brunk, B. P., Dommer, J., Fischer, S., Gajria, B., Gao, X., Gingle, A.,  
474 Grant, G., Harb, O. S., Heiges, M., Innamorato, F., Iodice, J., Kissinger, J. C., Kraemer, E., Li, W.,  
475 Miller, J. A., Nayak, V., Pennington, C., ... Wang, H. (2008). PlasmoDB: a functional genomic



- 476 database for malaria parasites. *Nucleic Acids Research*, 37(suppl\_1), D539–D543.  
477 <https://doi.org/10.1093/nar/gkn814>
- 478 Balbin, C. A., Nunez-Castilla, J., Stebliankin, V., Baral, P., Sobhan, M., Cickovski, T., Mondal, A.  
479 M., Narasimhan, G., Chapagain, P., Mathee, K., & Siltberg-Liberles, J. (2023). Epitopedia:  
480 Identifying molecular mimicry between pathogens and known immune epitopes. *ImmunoInformatics*,  
481 9, 100023. <https://doi.org/10.1016/j.immuno.2023.100023>
- 482 Buchfink, B., Reuter, K., & Drost, H.-G. (2021). Sensitive protein alignments at tree-of-life scale  
483 using DIAMOND. *Nature Methods*, 18(4), 366–368. <https://doi.org/10.1038/s41592-021-01101-x>
- 484 Cameron, C. M., Barrett, J. W., Mann, M., Lucas, A., & McFadden, G. (2005). Myxoma virus  
485 M128L is expressed as a cell surface CD47-like virulence factor that contributes to the  
486 downregulation of macrophage activation in vivo. *Virology*, 337(1), 55–67.  
487 <https://doi.org/10.1016/j.virol.2005.03.037>
- 488 Cerami, C., Frevert, U., Sinnis, P., Takacs, B., Clavijo, P., Santos, M. J., & Nussenzweig, V. (1992).  
489 The basolateral domain of the hepatocyte plasma membrane bears receptors for the circumsporozoite  
490 protein of *Plasmodium falciparum* sporozoites. *Cell*, 70(6), 1021–1033.
- 491 Chulanetra, M., & Chaicumpa, W. (2021). Revisiting the Mechanisms of Immune Evasion Employed  
492 by Human Parasites. *Frontiers in Cellular and Infection Microbiology*, 11.  
493 <https://doi.org/10.3389/fcimb.2021.702125>
- 494 Damian, R. T. (1964). Molecular mimicry: Antigen sharing by parasite and host and its  
495 consequences. *The American Naturalist*, 98(900), 129–149.
- 496 De, A., Tiwari, A., Pande, V., & Sinha, A. (2022). Evolutionary trilogy of malaria, angiotensin II and  
497 hypertension: Deeper insights and the way forward. *Journal of Human Hypertension*, 36(4), 344–  
498 351. <https://doi.org/10.1038/s41371-021-00599-0>

- 499 Dolan, P. T., Roth, A. P., Xue, B., Sun, R., Dunker, A. K., Uversky, V. N., & LaCount, D. J. (2015).  
500 Intrinsic disorder mediates hepatitis C virus core-host cell protein interactions. *Protein Science : A*  
501 *Publication of the Protein Society*, 24(2), 221–235. <https://doi.org/10.1002/pro.2608>
- 502 Doxey, A. C., & McConkey, B. J. (2013). Prediction of molecular mimicry candidates in human  
503 pathogenic bacteria. *Virulence*, 4(6). <https://doi.org/10.4161/viru.25180>
- 504 Emms, D. M., & Kelly, S. (2019). OrthoFinder: Phylogenetic orthology inference for comparative  
505 genomics. *Genome Biology*, 20(1), 238. <https://doi.org/10.1186/s13059-019-1832-y>
- 506 Garg, A., Dabburu, G. R., Singhal, N., & Kumar, M. (2022). Investigating the disordered regions  
507 (MoRFs, SLiMs and LCRs) and functions of mimicry proteins/peptides in silico. *PLOS ONE*, 17(4),  
508 1–11. <https://doi.org/10.1371/journal.pone.0265657>
- 509 Garg, S., Shivappagowdar, A., Hada, R. S., Ayana, R., Bathula, C., Sen, S., Kalia, I., Pati, S., Singh,  
510 A. P., & Singh, S. (2020). Plasmodium Perforin-Like Protein Pores on the Host Cell Membrane  
511 Contribute in Its Multistage Growth and Erythrocyte Senescence. *Frontiers in Cellular and Infection*  
512 *Microbiology*, 10. <https://www.frontiersin.org/articles/10.3389/fcimb.2020.00121>
- 513 Georgiev, H., Ravens, I., Papadogianni, G., & Bernhardt, G. (2018). Coming of Age: CD96 Emerges  
514 as Modulator of Immune Responses. *Frontiers in Immunology*, 9.  
515 <https://www.frontiersin.org/articles/10.3389/fimmu.2018.01072>
- 516 Getts, D. R., Chastain, E. M. L., Terry, R. L., & Miller, S. D. (2013). Virus infection, antiviral  
517 immunity, and autoimmunity. *Immunological Reviews*, 255(1), 197–209.  
518 <https://doi.org/10.1111/imr.12091>
- 519 Harrison, T. E., Mørch, A. M., Felce, J. H., Sakoguchi, A., Reid, A. J., Arase, H., Dustin, M. L., &  
520 Higgins, M. K. (2020). Structural basis for RIFIN-mediated activation of LILRB1 in malaria. *Nature*,  
521 587(7833), 309–312. <https://doi.org/10.1038/s41586-020-2530-3>

- 522 Hebert, F. O., Phelps, L., Samonte, I., Panchal, M., Grambauer, S., Barber, I., Kalbe, M., Landry, C.  
523 R., & Aubin-Horth, N. (2015). Identification of candidate mimicry proteins involved in parasite-  
524 driven phenotypic changes. *Parasites & Vectors*, 8, 225. <https://doi.org/10.1186/s13071-015-0834-1>
- 525 Holm, L. (2022). *Dali server: Structural unification of protein families*. 50(May), 210–215.
- 526 Ji, C., Shen, H., Su, C., Li, Y., Chen, S., Sharp, T. H., & Xiao, J. (2022). Plasmodium falciparum has  
527 evolved multiple mechanisms to hijack human immunoglobulin M. *BioRxiv*.
- 528 Kennedy, A. T., Kennedy, A. T., Schmidt, C. Q., Thompson, J. K., Weiss, G. E., Taechalertpaisarn,  
529 T., Gilson, P. R., Barlow, P. N., Crabb, B. S., Cowman, A. F., & Tham, W. (2016). *Recruitment of*  
530 *Factor H as a Novel Complement Evasion Strategy for Blood-Stage*. 196, 1239–1248.  
531 <https://doi.org/10.4049/jimmunol.1501581>
- 532 Kvensakul, M., van Delft, M. F., Lee, E. F., Gulbis, J. M., Fairlie, W. D., Huang, D. C. S., &  
533 Colman, P. M. (2007). A Structural Viral Mimic of Prosurvival Bcl-2: A Pivotal Role for  
534 Sequestering Proapoptotic Bax and Bak. *Molecular Cell*, 25(6), 933–942.  
535 <https://doi.org/10.1016/j.molcel.2007.02.004>
- 536 Leshchyn'ska, I., & Sytnyk, V. (2016). Reciprocal Interactions between Cell Adhesion Molecules of  
537 the Immunoglobulin Superfamily and the Cytoskeleton in Neurons. *Frontiers in Cell and*  
538 *Developmental Biology*, 4. <https://doi.org/10.3389/fcell.2016.00009>
- 539 Ludin, P., Nilsson, D., & Mäser, P. (2011). Genome-Wide Identification of Molecular Mimicry  
540 Candidates in Parasites. *PLOS ONE*, 6(3), e17546.
- 541 Lyons, F. M. T., Gabriela, M., Tham, W., Dietrich, M. H., & Craig, A. (2022). *Plasmodium 6-*  
542 *Cysteine Proteins: Functional Diversity , Transmission- Blocking Antibodies and Structural*  
543 *Scaffolds*. 12(July), 1–20. <https://doi.org/10.3389/fcimb.2022.945924>

- 544 Monzon, V., Paysan-Lafosse, T., Wood, V., & Bateman, A. (2022). Reciprocal best structure hits:  
545 Using AlphaFold models to discover distant homologues. *Bioinformatics Advances*, 2(1).  
546 <https://doi.org/10.1093/bioadv/vbac072>
- 547 Mousa, A. A., Roche, D. B., Terkawi, M. A., Kameyama, K., Kamyngkird, K., Vudriko, P., Salama,  
548 A., Cao, S., Orabi, S., Khalifa, H., Ahmed, M., Attia, M., Elkirdasy, A., Nishikawa, Y., Xuan, X., &  
549 Cornillot, E. (2017). Human babesiosis: Indication of a molecular mimicry between thrombospondin  
550 domains from a novel Babesia microti BmP53 protein and host platelets molecules. *PLOS ONE*,  
551 12(10), e0185372. <https://doi.org/10.1371/journal.pone.0185372>
- 552 Oliver-González, J. (1944). The Inhibition of Human Isoagglutinins by a Polysaccharide from  
553 *Ascaris Suum*. *The Journal of Infectious Diseases*, 74(2), 81–84.  
554 <https://doi.org/10.1093/infdis/74.2.81>
- 555 Oyong, D., Piera, K. A., Barber, B. E., William, T., Eisen, D. P., Minigo, G., Langer, C., Drew, D.  
556 R., Rivera, F. D. L., Amante, F. H., Williams, T. N., Kinyanjui, S., & Marsh, K. (2019). *IgM in*  
557 *human immunity to Plasmodium falciparum malaria*. September.
- 558 Paul, G., Deshmukh, A., Kaur, I., Rathore, S., Dabral, S., Panda, A., Singh, S. K., Mohammed, A.,  
559 Theisen, M., & Malhotra, P. (2017). A novel Pfs38 protein complex on the surface of Plasmodium  
560 falciparum blood - stage merozoites. *Malaria Journal*, 1–15. [https://doi.org/10.1186/s12936-017-](https://doi.org/10.1186/s12936-017-1716-0)  
561 1716-0
- 562 Pickard, M. R., Mourtada-Maarabouni, M., & Williams, G. T. (2011). Candidate tumour suppressor  
563 Fau regulates apoptosis in human cells: An essential role for Bcl-G. *Biochimica et Biophysica Acta*,  
564 1812(9), 1146–1153. <https://doi.org/10.1016/j.bbadis.2011.04.009>

- 565 Pleass, R. J., Moore, S. C., Stevenson, L., & Hviid, L. (2016). Immunoglobulin M : Restrainer of In fl  
566 ammation and Mediator of Immune Evasion by Plasmodium falciparum Malaria. *Trends in*  
567 *Parasitology*, 32(2), 108–119. <https://doi.org/10.1016/j.pt.2015.09.007>
- 568 Ragotte, R. J., Higgins, M. K., & Draper, S. J. (2020). The RH5-CyRPA-Ripr Complex as a Malaria  
569 Vaccine Target. *Trends in Parasitology*, 36(6), 545–559. <https://doi.org/10.1016/j.pt.2020.04.003>
- 570 Remarque, E. J., Faber, B. W., Kocken, C. H. M., & Thomas, A. W. (2008). Apical membrane  
571 antigen 1: A malaria vaccine candidate in review. *Trends in Parasitology*, 24(2), 74–84.  
572 <https://doi.org/10.1016/j.pt.2007.12.002>
- 573 Robson, K. J. H., Hall, J. R. S., Jennings, M. W., Harris, T. J. R., Marsh, K., Newbold, C. I., Tate, V.  
574 E., & Weatherall, D. J. (1988). A highly conserved amino-acid sequence in thrombospondin,  
575 properdin and in proteins from sporozoites and blood stages of a human malaria parasite. *Nature*,  
576 335(6185), 79–82.
- 577 Ronneberger, O., Tunyasuvunakool, K., Bates, R., Židek, A., Ballard, A. J., Cowie, A., Romera-  
578 paredes, B., Nikolov, S., Jain, R., Adler, J., Back, T., Petersen, S., Reiman, D., Clancy, E., Zielinski,  
579 M., Steinegger, M., Pacholska, M., Berghammer, T., Bodenstein, S., ... Kavukcuoglu, K. (2021).  
580 Highly accurate protein structure prediction with AlphaFold. *Nature*, 596(May).  
581 <https://doi.org/10.1038/s41586-021-03819-2>
- 582 Sallee, N. A., Rivera, G. M., Dueber, J. E., Vasilescu, D., Mullins, R. D., Mayer, B. J., & Lim, W. A.  
583 (2008). The pathogen protein EspFU hijacks actin polymerization using mimicry and multivalency.  
584 *Nature*, 454(7207), 1005–1008. <https://doi.org/10.1038/nature07170>
- 585 Schmaier, A. H. (2003). The kallikrein-kinin and the renin-angiotensin systems have a multilayered  
586 interaction. *American Journal of Physiology-Regulatory, Integrative and Comparative Physiology*,  
587 285(1), R1–R13. <https://doi.org/10.1152/ajpregu.00535.2002>

- 588 Tayal, S., Bhatia, V., Mehrotra, T., & Bhatnagar, S. (2022). ImitateDB: A database for domain and  
589 motif mimicry incorporating host and pathogen protein interactions. *Amino Acids*, *54*(6), 923–934.  
590 <https://doi.org/10.1007/s00726-022-03163-3>
- 591 van Kempen, M., Kim, S. S., Tumescheit, C., Mirdita, M., Gilchrist, C. L. M., Söding, J., &  
592 Steinegger, M. (2022). Foldseek: Fast and accurate protein structure search. *BioRxiv*,  
593 2022.02.07.479398. <https://doi.org/10.1101/2022.02.07.479398>
- 594 Wasmuth J. D., Pszenny V., Haile S., Jansen E. M., Gast A. T., Sher A., Boyle J. P., Boulanger M. J.,  
595 Parkinson J., & Grigg M. E. (2012). Integrated Bioinformatic and Targeted Deletion Analyses of the  
596 SRS Gene Superfamily Identify SRS29C as a Negative Regulator of Toxoplasma Virulence. *MBio*,  
597 *3*(6), e00321-12. <https://doi.org/10.1128/mBio.00321-12>
- 598 Weisman, C. M., Murray, A. W., & Eddy, S. R. (2020). Many, but not all, lineage-specific genes can  
599 be explained by homology detection failure. *PLOS Biology*, *18*(11), e3000862.  
600 <https://doi.org/10.1371/journal.pbio.3000862>
- 601 Westphal, D., Ledgerwood, E. C., Hibma, M. H., Fleming, S. B., Whelan, E. M., & Mercer, A. A.  
602 (2007). A novel Bcl-2-like inhibitor of apoptosis is encoded by the parapoxvirus ORF virus. *Journal*  
603 *of Virology*, *81*(13), 7178–7188. <https://doi.org/10.1128/JVI.00404-07>
- 604 Wheeler, R. J. (2021). A resource for improved predictions of Trypanosoma and Leishmania protein  
605 three-dimensional structure. *PLOS ONE*, *16*(11), 1–12. <https://doi.org/10.1371/journal.pone.0259871>
- 606 Wichers, J. S., Scholz, J. A. M., Strauss, J., Witt, S., Lill, A., Ehnold, L.-I., Neupert, N., Liffner, B.,  
607 Lühken, R., Petter, M., Lorenzen, S., Wilson, D. W., Löw, C., Lavazec, C., Bruchhaus, I., Tannich,  
608 E., Gilberger, T. W., & Bachmann, A. (2019). Dissecting the Gene Expression, Localization,  
609 Membrane Topology, and Function of the Plasmodium falciparum STEVOR Protein Family. *MBio*,  
610 *10*(4). <https://doi.org/10.1128/mBio.01500-19>

- 611 Wolf, A.-S., Sherratt, S., & Riley, E. M. (2017). NK Cells: Uncertain Allies against Malaria.  
612 *Frontiers in Immunology*, 8. <https://www.frontiersin.org/articles/10.3389/fimmu.2017.00212>
- 613 Wu, Y. (2015). Contact pathway of coagulation and inflammation. *Thrombosis Journal*, 13(1), 17.  
614 <https://doi.org/10.1186/s12959-015-0048-y>
- 615 Xue, B., Blocquel, D., Habchi, J., Uversky, A. V., Kurgan, L., Uversky, V. N., & Longhi, S. (2014).  
616 Structural disorder in viral proteins. *Chemical Reviews*, 114(13), 6880–6911.  
617 <https://doi.org/10.1021/cr4005692>
- 618 Zanghì, G., Vembar, S. S., Baumgarten, S., Ding, S., Guizetti, J., Bryant, J. M., Mattei, D., Jensen, A.  
619 T. R., Rénia, L., Goh, Y. S., Sauerwein, R., Hermsen, C. C., Franetich, J.-F., Bordessoulles, M.,  
620 Silvie, O., Soulard, V., Scatton, O., Chen, P., Mecheri, S., ... Scherf, A. (2018). A Specific PfEMP1  
621 Is Expressed in *P. falciparum* Sporozoites and Plays a Role in Hepatocyte Infection. *Cell Reports*,  
622 22(11), 2951–2963. <https://doi.org/10.1016/j.celrep.2018.02.075>

623

## 624 **12 Data Availability Statement**

625 Supplementary materials for this study have been deposited in the Open Science Framework  
626 repository at Muthye, V., & Wasmuth, J. (2023, February 9). Data for Proteome-wide comparison of  
627 tertiary protein structures reveal extensive molecular mimicry in Plasmodium-human interactions.”  
628 <https://doi.org/10.17605/OSF.IO/CUSYG>